Laser and Particle Beams (2005), *23*, 79–85. Printed in the USA.

DOI: 10.1017/S0263034605050147

Radiation dynamics of fast heavy ions interacting with matter

O.N. ROSMEJ,[1] S.A. PIKUZ, JR.,[2] S. KOROSTIY,[1] A. BLAZEVIC,[3] E. BRAMBRINK,[3] A. FERTMAN,[4] T. MUTIN,[4] V.P. EFREMOV,[2] T.A. PIKUZ,[5] A.YA. FAENOV,[5] P. LOBODA,[6] A.A. GOLUBEV,[4] AND D.H.H. HOFFMANN[1,3]

[1]Gesellschaft für Schwerionenforschung, GSI, Department of Plasma Physics, Darmstadt, Germany
[2]Institute for High Energy Density, Russian Academy of Sciences, Moscow, Russia
[3]Technical University, Darmstadt, Germany
[4]Institute of Experimental and Theoretical Physics, Moscow, Russia
[5]Multicharged Ions Spectra Data Center, All Russian Institute of Technical Physics, Mendeleevo, Russia
[6]Russian Federal Nuclear Center, All Russian Institute of Technical Physics, Chelyabinsk, Russia

(RECEIVED 10 September 2004; ACCEPTED 28 October 2004)

Abstract

The study of heavy ion stopping dynamics using associated K-shell projectile and target radiation was the focus of the reported experiments. Ar, Ca, Ti, and Ni projectile ions with the initial energies of 5.9 and 11.4 MeV/u were slowed down in quartz and arogels. Characteristic radiation of projectiles and target atoms induced in close collisions was registered. The variation of the projectile ion line Doppler shift due to the ion deceleration measured along the ion beam trajectory was used to determine the ion velocity dynamics. The dependence of the ion velocity on the trajectory coordinate was measured over 70–90% of the ion beam path with a spatial resolution of 50–70 μm. The choice of SiO_2 aerogel with low mean densities of 0.04–0.15 g/cm^3 as a target material, made it possible to stretch the ion stopping range by more than 20–50 times in comparison with solid quartz. It allowed for resolving the dynamics of the ion stopping process. Experimentally, it has been proven that the fine porous nano-structure of aerogels does not affect the ion energy loss and charge state distribution. The strong increase of the ion stopping range in aerogels made it possible to resolve fast ion radiation dynamics. The analysis of the projectile Kα-satellites structure allows supposing that ions propagate in solid in highly exicted states. This can provide an experimental explanation for so called gas-solid effect.

Keywords: Doppler shift; Energetic ions; Ion-stopping power; K-shell radiation; X-ray spectroscopy

1. INTRODUCTION

At the first stage of the heavy ion fusion (HIF) scenario, energetic ion beams irradiate a cold solid or porous target to high temperature and to initiate the conversion of the deposited ion beam energy into energetic photons (Dolgoleva *et al*., 2003; Kawata *et al*., 2003). During the interaction time, the heated target material undergoes subsequent phase transitions into liquid, gaseous, and plasma states (Tahir *et al*., 2003; Hoffmann *et al*., 2005). Variations of the target material properties such as density and degree of ionization can influence the ion stopping power significantly.

The influence of the target density on the projectile ion stopping process was pointed out by Lassen (1951) in his investigations of fission fragments passing through various gaseous and solid targets. It was found that the mean charge of fast ions passing through gaseous targets is lower than those after solids with the same linear density.

Systematically this effect was studied by Geissel *et al*. (1982) and Bimbot *et al*. (1989). Experiments on the ion beam; plasma interaction discovered effects like a drastically increase in the stopping power, and the mean charge state of ions in fully ionized discharge plasma (Hoffmann *et al*., 1990; Dietrich, 1992; Hasegawa *et al*., 2003). The classical approach to the ion stopping phenomena (Bohr–Bethe–Bloch) neglects the projectile internal structure and considers it to be a point charge. But such phenomena as a temporal evolution of ion charge states, target density effect, and stopping in partially ionized matter (Mintsev *et al*., 1999; Roth *et al*., 2000), cannot be understood without detailed knowledge about projectile subshell population dynamics during the stopping process.

Address correspondence and reprint requests to: O. N. Rosmej, Gesellschaft für Schwerionenforschung (GSI), Department of Plasma Physics, Planckstrasse 1, 64291 Darmstadt, Germany. E-mail: o.rosmej@gsi.de

Bohr and Lindhard (1954) and Betz and Grodzins (1975) underlined an important role of projectile excited electrons, considering the influence of the target density on the ion stopping power. Anholt (1984) examined analytically the influence of projectile excited states on the equilibrium charge state of relativistic heavy ions with $Z < 20$ in solids. Peter and Meyer-ter-Vehn (1991) studied time dependent population kinetics of the projectile ground states in the ionized matter. In fully ionized matter, a drastic decrease of recombination rates causes the increase of the projectile charge and consequently causes the ion stopping power to rise. Moreover, it prolongs the time needed to reach the equilibrium in ion charge state distribution at low ion energies, thus one has to take into account as well non-equilibrium effects.

However, in experiments, the most important parameter such as the projectile charge state distribution is usually measured after the ions have left the interaction volume. In a vacuum, during the time of 10–100 fs, the ion charge state distribution and electron distribution over projectile exited states can be changed due to collisionless processes like Auger effect, and spontaneous radiative decay to the projectile ground state.

In the present experiments, we made use of K-shell radiative transitions of multi charged energetic ions for the determination of the projectile charge state distribution and velocity along the trajectory, directly from the interaction volume. The charge state of energetic ions passing through matter fluctuates due to electron capture and loss processes which occur with high probabilities in ion-atom collisions. In general, probabilities of these processes depend on the velocity, charge, and electron configuration of the projectile, nuclear charge and density of the target material. Radiative deexcitation of the excited states gives rise to the projectile and target atom characteristic emission.

Due to the shielding effects, produced by bound projectile electrons, the energies of the K-shell radiative transitions vary slightly with the ion charge. This allows us to observe all possible projectile charge state simultaneously and to follow the dynamic of ion charge state distribution caused by the stopping process. The relative line intensities of Kα-satellites—(1s ml^k −2p ml^k, $k = 0, Z_{\mathrm{nuc}} - 1$) reflect the charge state distribution of projectile ions. The variation of the Doppler shift of the projectile radiation due to the ion deceleration, measured with a high spatial resolution is used to determine the ion velocity dynamics. Therefore, the applied method is capable of giving the most important information for the stopping theory; the dynamical relationship between the ion charge and velocity along the ion trajectory during the slowing down process.

2. EXPERIMENT

Experiments on the interaction of heavy ion beams with cold matter were carried out at the linear accelerator, UNILAC, Gesellschaft fuer Schwerionenforschung mbH (GSI, Darmstadt, Germany). The aims were to receive space resolved information on the projectile charge and velocity during the stopping process. Ar, Ca, Ti, and Ni projectiles, with energies of 5.9 and 11.4 MeV/u were stopped in different media: quartz and porous SiO_2 aerogels (Rosmej *et al.*, 2002). Associated K-shell radiation caused by inelastic collisions of heavy ions penetrating thick solid targets was measured.

The principal scheme of the spectra registration is shown in Fig. 1. The ion beam was delivered to the vacuum chamber with typical focusing spot dimension on the target from 1 to 2 mm. The usual ion beam current was varied from 1 to 4 μA in experiments, where solid quartz was used as a target material and in the range of 0.1–0.5 μA for aerogel targets. X-ray emission caused by ion-target atom inelastic collisions in the interaction zone was registered by means of focusing spectrometers with spatial resolution (FSSR) (Faenov *et al.*, 1994).

The FSSR design utilizes two aspects: (1). The Bragg crystal X-ray diffraction low in the plane of dispersion:

$$\lambda m = 2d_m \sin\Theta, \tag{1}$$

where λ is the wavelength, m is the reflection order, d_m is the interplanar distance of the crystal for m-th order of reflection, and Θ is the Bragg angle for the central wavelength; (2). The spherical mirror low in the sagittal plane described by:

$$1/a + 1/b = 2\sin\Theta/R, \tag{2}$$

where R is the radius of curvature of the spherical surface, a is the distance between the source and the mirror (in our case the crystal), and b is the distance from the mirror to the object plane (film or X-ray detector). As disperse elements spherically bent mica and quartz crystals with radii of curvature $R = 150$ mm and apertures 15×50 mm^2 were used.

In our experiments, spatially resolved Kα-spectra of Ar, Ca, Ti, and Ni projectile ions, as well as of the stopping media have been recorded. To distinguish Kα-radiation caused by different ion charges spectral resolution $\lambda/\delta\lambda \geq 1000$ is required. The spectral resolution achieved in experiments was $\lambda/\Delta\lambda = 3000$. Spectra were observed with a spatial resolution of 50–70 μkm in the direction of the ion beam propagation.

The spatial resolution (up to 50–70 μm). Spectra were observed with a spatial resolution in the direction of the ion beam propagation. Radiation was recorded using KODAC DEF-5 X-ray films. The exposure time needed to accumulate the X-ray signal in experiments with aerogel targets was typically 5–7 hours. It corresponds to a projectile ion fluency of about 10^{13} ion/sm^2. Due to the optical properties of the spherical bent crystals, the length of spectral lines at the detector corresponds to the magnified length of the interaction zone (see Fig. 1).

Figure 2 shows Kα-radiation of 5.9 MeV/u Ni-ions slowing down in thick quartz plate of 2.23 g/cm^3 density. The

https://doi.org/10.1017/S0263034605050147 Published online by Cambridge University Press

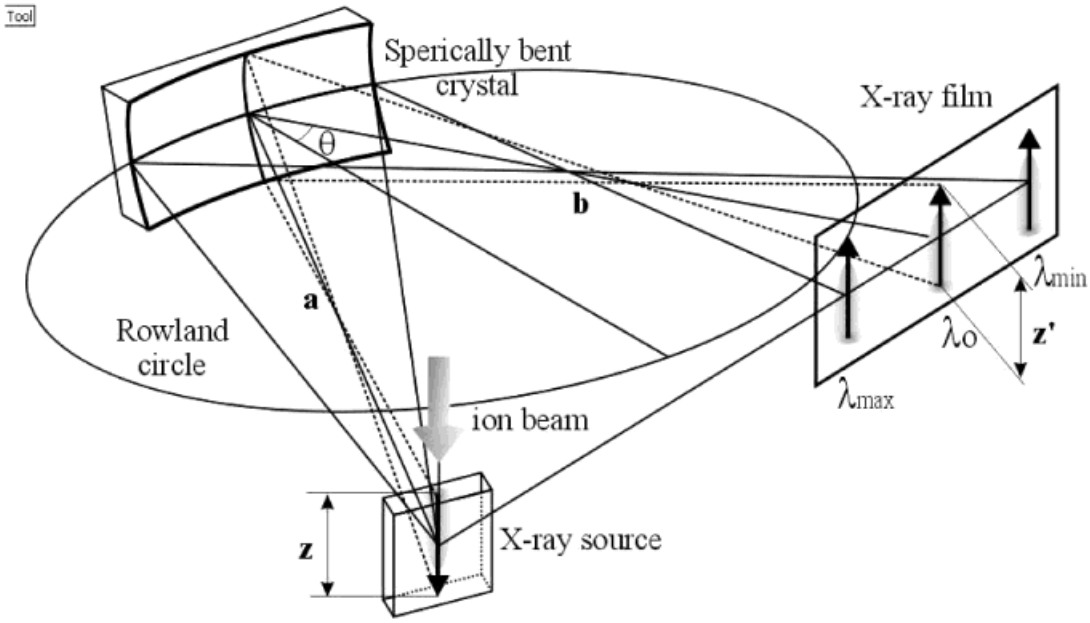

Fig. 1. Principal registration scheme with spherically bent crystal spectrometer.

stopping length of a swift heavy ion depends on its energy and characteristics of the target media.

The stopping length of Ni ions with this initial energy in solids is very short (up to 50 μm). In this case, spatially resolved measurements are practically impossible.

To stretch the ion-stopping path, a new type of target material was used. Silica aerogel is a transparent porous material. Its structure is formed by chains of colloidal SiO_2–beads of 1–10 nm in diameter.

The chains build a three-dimensional open cell structure, like a sponge, with pores less than 30–50 nm (Borisenko & Merkuliev, 1996; Demidov *et al.*, 1998; Borisenko *et al.*, 2003).

The nm uniform aerogel structure provides a continuously expanded interaction volume with small spatial gradients. The wide variety of aerogel mean densities (0.02–0.5 g/cm^3) allows stretching of the ion stopping length up to 100 times in comparison with solid quartz, and reaching high

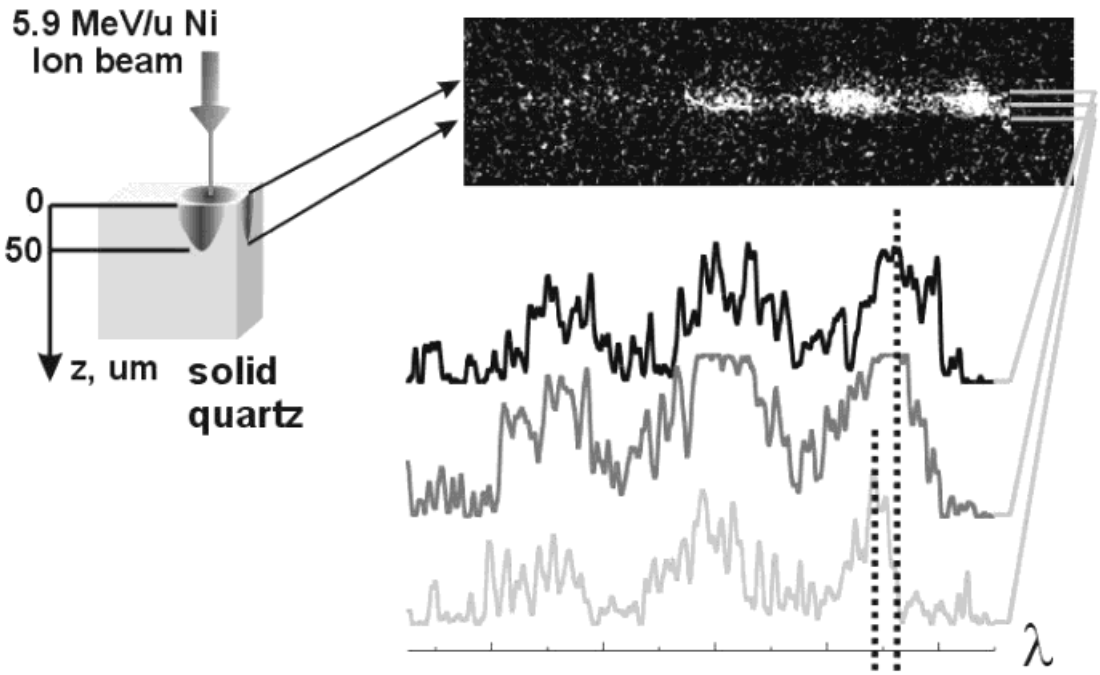

Fig. 2. K-shell radiation of 5.9 MeV/u Ni ions penetrating thick quartz target.

https://doi.org/10.1017/S0263034605050147 Published online by Cambridge University Press

spatial resolution of the ion radiation dynamics. The porous structure will not influence the projectile charge state distribution provided the time of flight of the ion inside the pore in a vacuum is shorter than the time scale of the radiative- and Auger-processes, which lead to the collision less relaxation of the projectile excited states. The important advantage of this material is the high transparency for X-rays.

To investigate the possible influence of the aerogel porous nano-sracture on the stopping process, the ion energy loss, and charge state distribution of 11.4 MeV/u Ar ion beam, interacting with 50 μm Al foil and 3 mm aerogel target with approximately the same linear densities were measured. For energy loss measurements time-of-flight method was used. As a result, 11.45 MeV/u Argon beam energy losses in 3 mm 0.04 g/cc aerogel target, and in Al foil of 50 $\pm$ 1 μm thickness have been determined and come to 3.40 $\pm$ 0.07 MeV/u, 3.16 $\pm$ 0.07 MeV/u. This result is in a good agreement with SRIM-calculated value of 3.20 $\pm$ 0.07 MeV/u.

Together with energy loss measurements, the analysis of charge state distribution after the target was carried out. After interaction with the investigated target, the beam burst is deflected in the magnetic field of a dipole magnet according to the ion charge to the momentum ratio q/mv.

Since the beam energy after a target was measured undependably, the charge state distribution in the ion beam can be determined (Fig. 3). Measured average charge states of Argon ions are: Z = 16.9 after Al foil and Z = 16.8 after aerogel. These results proved that at our experimental conditions, the pore of 30–50 nm sizes does not seriously influence the ion stopping processes.

In experiments on the interaction of fast ions with aerogels, K-shell projectile and target radiation was registered. Figure 4 demonstrates Kα-spectra of Si–target atoms under influence of 5.9 MeV/u Ni ion beam. As a target, a 6 mm thick piece of SiO_2-gel with the density of 0.15 g/cm^3 was used. Due to low mean density, the Ni ion stopping length was stretched up to 900 μm. The picture shows an X-ray image of the interaction zone dispersed in characteristic lines of Si.

Due to the very high ionization potential of the Si K-shell (2.3–2.6 keV), ionization of 1s electrons can be induced only in close ion-atom collisions. This leads to additional ionization of M- and L-shell target electrons (Kaufmann *et al.*, 1976). In the target K-shell spectrum, we can observe the radiative transitions in highly ionized Si ions up to Li-like charge state as well as Kα line accumulating transitions in Si ions having M-shell electrons. In this experiments, spectral resolution of $\lambda/\delta\lambda = 3000$ was achieved.

The prominent features of the projectile ion spectra (see Fig. 5a, 5b) are the presence of the H-like Ly_α lines $1s^2S_{1/2} - 2p^2P_{1/2,3/2}$, the He-like resonance line He_α:$1s2p(^1P_1) - 1s^2(^1S_0)$ as well, the groups of satellites 1s2l-2l2l′ and $1s^22l$-1s2l2l′.

For elements heavier as Ti, one can record as well the radiation of intercombination line $1s2p(^3P_1) - 1s^2(^1S_0)$ (see Fig. 5a). At the projectile energy of 11.4 MeV/u the dielectronic satellites in spectra are less pronounced due to the low recombination cross sections at high ion velocities.

K-shell spectra of energetic ions recorded with a spatial resolution reveal very interesting features: (a) we observe intense long lasting radiation of H-, He-, and Li-like ion charge states over 70–80% of ion stopping length; (b) in contrast to the target K-shell spectra having vertical lines (see Fig. 4), projectile lines registered with a spatial resolution are tilted, demonstrating attenuation of the line Doppler shift due to the ion deceleration in stopping media.

This feature of the projectile K-shell spectra was used for calculations of the ion velocity inside the interaction volume. The following relativistic equation for the line Doppler shift was used:

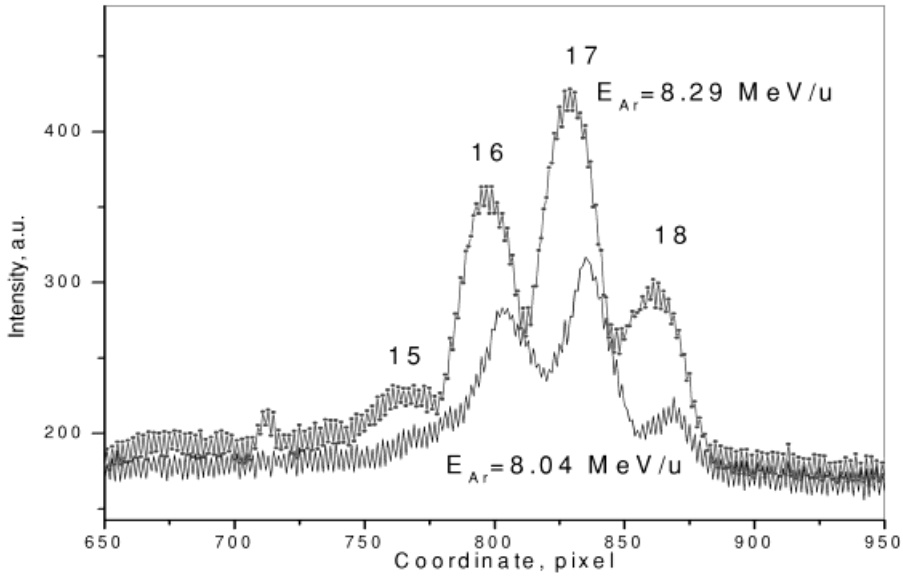

Fig. 3. Ar charge state distribution after penetrating of aerogel target with a linear density of 0.012g/cm^2 and Al target of 0.013g/cm^2.

https://doi.org/10.1017/S0263034605050147 Published online by Cambridge University Press

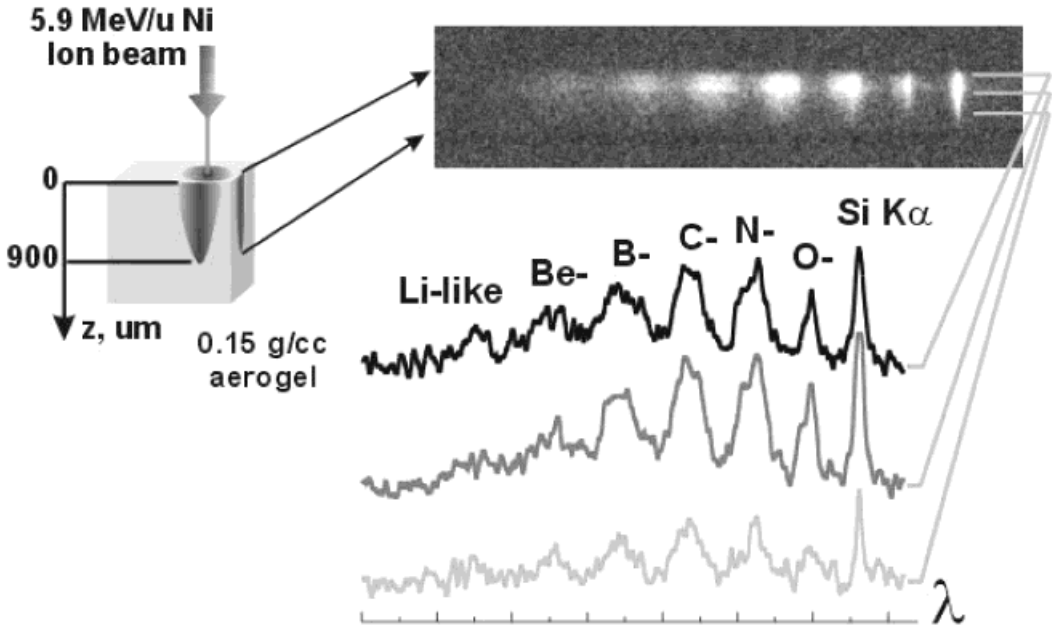

Fig. 4. Si-target Ka-spectra induced under 5.9 MeV/u Ni ion beam interacting with 0.15 g/cm^3 SiO_2 aerogel target.

$$\lambda_D = \lambda_0 \left(\frac{1}{\sqrt{1-\left(\frac{v}{c}\right)^2}} + \frac{\frac{v}{c}\cdot\sin\varphi}{\sqrt{1-\left(\frac{v}{c}\right)^2}} \right) \qquad (3)$$

where, λ_D is the measured wavelength, λ_0 is the wavelength of a radiative transition in the ion at rest, v is the projectile ion velocity, c is the speed of light, φ is the angle between normal to the direction of the ion beam propagation and the direction of observation.

From the space resolved analysis of the relative Doppler line shift $\delta\lambda_D$, the experimental dependence of the projectile velocity v on the depth of ion penetration x (Rosmej *et al.*, 2003) was found, see Fig. 6. In our calculations, we started with the assumption that the energy of ions at the beginning of Ly-α and He-α line emission v_{beam} corresponds to the initial ion beam energy in the accelerator. The accuracy of ion velocity measurements is determined by spectral and spatial resolution reached in experiment. Spatial resolution was not less than 70 μm. The method provided 2% of accuracy at the beginning of the ion stopping path and 20% at the end. The decrease of the accuracy at the end of the ion beam track is due to the low line intensities and broadening of ion beam energy profile in the stopping media.

The experimental data were compared with the numerical calculations of the energy losses using the open semi-empirical SRIM code (www.srim.org). The comparison shows a good coincidence between the measured and calculated stop-

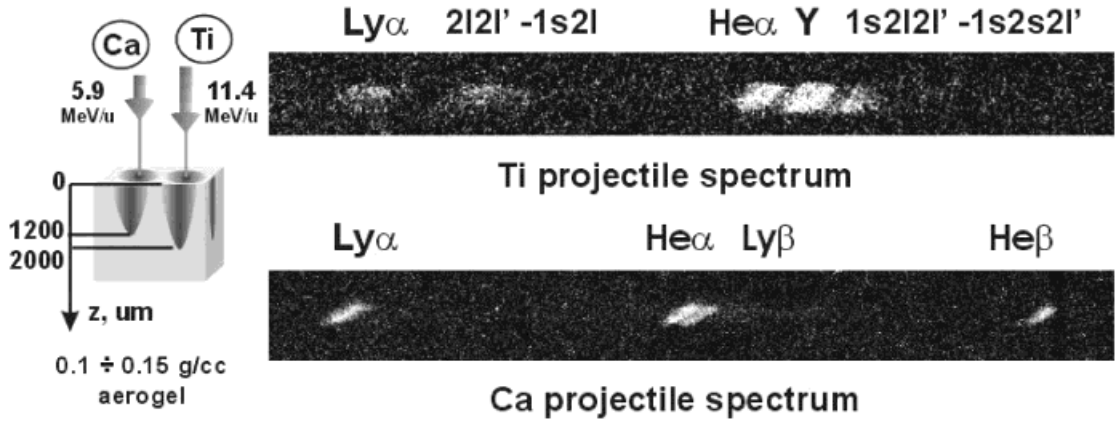

Fig. 5. (a) Ti^{11+} ions ($E = 11.4$ MeV/u) interacting with silica aerogel ($\rho = 0.1$ g/cm^3) (b) Ca^{9+} ions ($E = 5.9$ MeV/u) interacting with silica aerogel ($\rho = 0.15$ g/cm^3).

https://doi.org/10.1017/S0263034605050147 Published online by Cambridge University Press

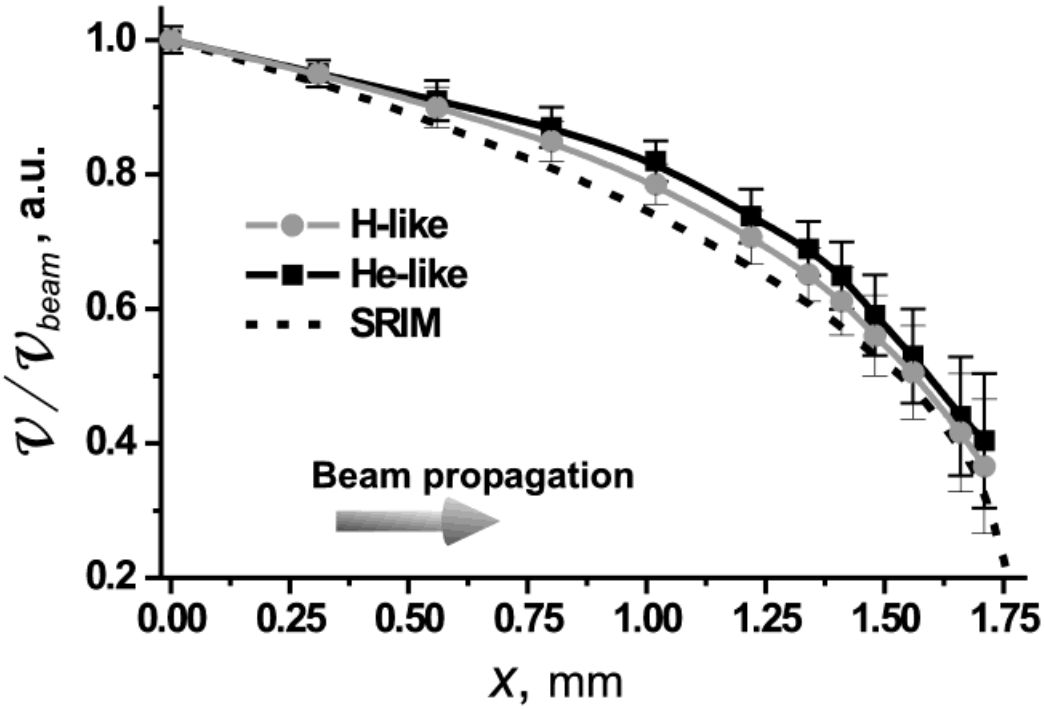

Fig. 6. Measured and calculated Ca-projectile ion velocity dynamics in aerogel.

ping dynamics of Ca ions in aerogels. The absolute shift between two curves seems to be systematic and occurs in experiments with another type of projectile ions. The reason could be as follow: due to the long exposition time needed for spectra accumulation, the aerogel surface gets to be damaged. Craters with the depth of 50–70 μm were measured after 5–7 hours of exposition under the ion beam. To improve the situation and decrees the exposition time, the X-ray CCD-camera shall be used instead of X-ray films.

The final projectile energy estimated using the method of Doppler shift attenuation from the spatially resolved K-shell spectra is about 1.5–3 MeV/u depending on the nuclear charge of the projectile. At these energies one would expect that the radiation of H- and He-like ions will disappear due to increase of recombination cross sections at low projectile energies (Shima *et al.*, 1992). As explanations for this effect we propose a suppression of bound electron capture in dense solid matter considered theoretically by Shevelko (Shevelko *et al.*, 2004).

Target bound electrons captured on the projectile excited states will be ionized with a high probability due to the high frequency collisions of about $v = 10^{16}$ Hz with target atoms. In the case of Ar and Ca ions, these collision rates in solids are higher than radiative decay rates already for projectile bound electron states with a quantum number $n = 2$ ($v < 10^{15}$–10^{14} Hz). The capture process on these levels cannot be stabilized via radiative decay cascade to the ground state. So, the electron structure of the projectile moving in solids consists of a "core" charge surrounded by the cloud of highly excited electrons. The highly excited electron structure can change the effective ion charge in matter. After emerging from the target no collisions take place and highly excited electrons undergo radiative decay to the ground states or Auger effect. The projectile charge state distribution usually measured after the ion leaves a target will be established.

Another situation will be expected in low density gaseous targets. There, radiative decay rates dominate over collisions and every act of electron capture is followed by radiative stabilization to the projectile ground state. Therefore, in low-density targets, ions propagate mostly in ground states and the ion charge state distribution established in stopping media will not be changed after the ion leaves the target. Therefore, the competition between collision and radiative processes influences the projectile bound electron structure and consequently effective ion charge in stopping media. This seems to be the main reason for the dependence of the ion stopping power on the density of the target material.

ACKNOWLEDGMENTS

The authors appreciate the fruitful discussions with C. Deutsch and G. Maynard, and a financial support of this collaborative work from German Ministry of Research and Development (BMBF), DAAD Leonard-Euler Stipendienprogramm, DFG–project 436 RUS 113/685/0-1 and NATO-PSR CLG 979372 project.

REFERENCES

Anholt, R. (1985). Atomic collisions with relativistic heavy ions. II. Light-ion charge states. *Phys. Rev. A* **31**, 3579.

Betz, H.D. & Grodzins, L. (1970). Charge states and excitation of fast heavy ions passing through solids: A new model for the density effect. *Phys. Rev. Lett.* **25**, 211–214.

Bimbot, R., Cabot, C., Gardes, D., Gauvin, H., Hingmann, R., Orliange, I., De Reilhac, L. & Hubert, F. (1989). Stopping power of gases for heavy ions: Gas-solid effect: I.2-13 MeV/u Ne and Ar projectiles. *NIM* **B 44**, 1–18.

Bohr, N. & Linhard, J. (1954). Electron capture and loss by heavy ions penetrating matter. *Kgl. Dansk. Videskab, Mat.-Fys. Medd.* **28**.

Borisenko, N.G. & Merkuliev, Ya.A. (1996). *Targets For Inertial Fusion*. Proceedings of P.N. Lebedev Institute. New York: Nova Science.

Borisenko, N.G., Akunets, A.A., Bushuev, V.S., Dorogotovtsev, V.M. & Merkuliev, Yu.A. (2003). Motivation and fabrication methods for inertial confinement fusion and inertial fusion energy targets. *Laser Part. Beams* **21**, 505–509.

Dolgoleva, G.V., Dovgaya, N.I., Nechpai, V.I., Kechin, V.I., Pevnaya, P.I., Sizova, L.I. & Knolin, S.A. (2003). Disk converter target. *Laser Part. Beams* **21**, 47–51.

Demidov, B.A., Efremov, V.P., Ivkin, M.V., Ivonin, I.A., Petrov, V.A. & Fortov, V.E. (1998). Determination of the dynamic characteristics of aerogels in the energy-release zone of a high-power electron beam. *Zhurnal Teknicheskoi Fiziki* **43**, 1239–1246.

Dietrich, K.-G., Hoffmann, D.H.H., Boggasch, E., Jacoby, J., Wahl, H., Elfers, M., Haas, C.R., Dubenkov, V.P. & Golubev, A.A. (1992). Charge state of fast heavy ions in a hydrogen plasma. *Phys. Rev. Lett.* **69**, 3623–3626.

Geissel, H., Laichter, Y., Schneider, W.F.W. & Ambruster, P. (1982). Observation of a gas-solid difference in the stopping powers of 1–10 MeV/u heavy ions. *Phys. Lett.* **88**, 26.

Hasegawa, J., Yokaya, N., Kobayashi, Y., Yoshida, M., Kojima, M., Sasaki, T., Fukuda, H., Ogawa, M., Oguri, Y. & Murakami, T. (2003). Stopping power of dense helium plasma for fast heavy ions. *Laser Part. Beams* **21**, 7–12.

Hoffmann, D.H.H., Blazevic, A., Ni, P., Rosmej, O., Roth, M., Tahir, N., Tauschwitz, A., Udrea, S., Varentsov, D., Weyrich, K. & Maron, Y. (2005). Present and future perspectives for high energy density physics with intense heavy ion and laser beams. *Laser Part. Beams* **23**, in print

Hoffmann, D.H.H., Weyrich, K., Wahl, H., Gardes, D., Bimbot, R. & Fleurier, C. (1990). Energy loss of heavy ions in a plasma target. *Phys. Rev. A* **42**, 2313–2321.

Faenov, A.Yu., Pikuz, S.A., Erko, A.I, Bryunetkin, I.A., Dyakin, V.M., Ivanenkov, G.V., Mingaleev, A.R., Pikuz, T.A., Romanova, V.M. & Shelkovenko, T.A. (1994). High-performance x-ray spectroscoopic devices for plasma micro-sources investigations. *Phys. Scr.* **50**, 333.

Kaufmann, R.L., Jamison, K.A., Gray, T.J. & Richard, P. (1976). Heavy-ion-produced high-resolution Si-K-x-ray spectra from a gas and solid. *Phys. Rev. Lett.* **36**, 1074.

Kawata, S., Someya, T., Nakamura, T., Miyazaki, S., Shimizu, K. & Ogoyski, A.I. (2003). Heavy ion beam final transport through an insulator guide in heavy ion fusion. *Laser Part. Beams* **21**, 27–32.

Lassen, N.O. (1951). The Total Charges of Fission Fragments in Gaseous and Solid Stopping Media. *Kgl. Dansk Videskab, Mat.-Fys. Medd* **26**.

Mintsev,V., Gryaznov, V., Kulish, M., Filimonov, A., Fortov, V., Sharkov, B., Golubev, A., Fertman, A., Turtikov, V., Kozodaev, A., Hoffmann, D.H.H., Funk, U. & Stoewe, S. (1999). Stopping power of proton beam in non-ideal plasma. *Contrib. Plasma Phys.* **37**, 101.

Peter, T. & Meyer-ter-Vehn, J. (1991). Energy loss of a heavy ions in dense plasma. II. Nonequilibrium charge states and stopping powers. *Phys. Rev. A* **43**, 2015–2030.

Rosmej, O.N., Wieser, J., Geissel, M., Rosmej, F., Blazevic, A., Jacoby, J., Dewald, E., Roth, M., Brambrink, E., Weyrich, K., Hoffmann, D.H.H., Pikuz, T.A., Faenov, A.Ya., Magunov, A.I., Skobelev, I.Yu., Borisenko, N.G., Shevelko, V.P., Golubev, A.A., Fertman, A., Turtikov, V. & Sharkov, B.Yu. (2002). X-ray spectromicroscopy of fast heavy ions and target radiation. *NIM A* **495**, 29.

Rosmej, O.N., Pikuz, Jr., S.A., Wieser, J., Blazevic, A., Brambrink, E., Roth, M., Efremov, V.P., Faenov, A.Ya., Pikuz, T.A., Skobelev, T.Yu. & Hoffmann, D.H.H. (2003). Investigation of the projectile ion velocity inside the interaction media by the x-ray spectromicroscopy method. *Rev. Sci. Instrum.* **74**, 5039.

Roth, M., Stöckl, C., Süss, W., Iwase, O., Gericke, O., Bock, R., Hoffmann, D.H.H., Geissel, M. & Seelig, W. (2000). Energy loss of heavy ions in laser-produced plasmas. *Europhys. Lett.* **50**, 28–34.

Shevelko, V.P., Rosmej, O.N., Tawara, H. & Tostikhina, I.Yu. (2004). Target-density effect in electron–capture process. *J. Phys.B* **37**, 201.

Shima, K., Kuno, N., Yamanouchi, M. & Tawara, H. (1992). Equilibrium fraction of ions of Z = 4-92 emerging from a carbon foil. *AD NDT* **51**, 173.

Tahir N.A., Shutov, S., Varentsov, D., Spiller, P., Udrea, S., Hoffmann, D.H.H., Lomonosov, I.V., Wieser, J., Kirk, M., Piriz, R., Fortov, V.E. & Bock, R. (2003). The influence of the equation of state of matter and ion beam characteristics on target heating and compression. *Phys. Rev. Spec. Top.* **6**, 020101.

https://doi.org/10.1017/S0263034605050147 Published online by Cambridge University Press